

Beyond Gross-Pitaevskii equation for 1D gas: quasiparticles and solitons

Jakub Kopyciński^{1*}, Maciej Lebek^{1,2}, Maciej Marciniāk¹, Rafał Ołdziejewski^{3,4}, Wojciech Górecki², Krzysztof Pawłowski¹

1 Center for Theoretical Physics, Polish Academy of Sciences, Al. Lotników 32/46, 02-668 Warsaw, Poland

2 Faculty of Physics, University of Warsaw, Pasteura 5, 02-093 Warsaw, Poland

3 Max Planck Institute of Quantum Optics, 85748 Garching, Germany

4 Munich Center for Quantum Science and Technology, Schellingstrasse 4, 80799 Munich, Germany

* jkopycinski@cft.edu.pl

July 17, 2022

Abstract

Describing properties of a strongly interacting quantum many-body system poses a serious challenge both for theory and experiment. In this work, we study elementary excitations of one-dimensional repulsive Bose gas for arbitrary interaction strength using a hydrodynamic approach. We use linearization to study type-I excitations and numerical minimization to study type-II excitations. We observe a good agreement between our approach and exact solutions of the Lieb-Liniger model for the particle modes and discrepancies for the hole modes. Therefore, the hydrodynamical equations find to be useful for long-wave structures and of a limited range of applicability for short-wave ones. We discuss potential further applications of our method.

Contents

1	Introduction	2
2	Models	4
3	Phonons and quasiparticles	7
4	Solitons	9
4.1	Comparison between solitons of GPE and LLGPE	9
4.2	Comparison between solitons and the type-II excitations	10
5	Validity range of LLGPE and solitons	13
6	Conclusions	14
A	Accurate approximations for e_{LL}	15

B Numerical implementation of dark solitons in (LL)GPE	15
References	16

1 Introduction

In a weakly interacting ultracold Bose gas, the mean-field approach given by a single particle non-linear Schrodinger equation, which is also known as the Gross-Pitaevski equation (GPE), has explained and predicted a large swathe of phenomena [1]. Interestingly, the GPE derives from the complete neglecting of the mutual correlations between the particles, and yet it describes non-linear phenomena that originate from interactions between them. The most known are solitons observed in experiments with an ultracold gas confined in a steep cigar-shaped harmonic trap [2–4]. In the repulsive gas, the solitons are density dips travelling with a constant speed, robust due to a balance between interaction and dispersion.

The original GPE, however, may overlook interesting physics even for weakly interacting systems with quantum depletion still being very small. In the presence of both repulsive and attractive interparticle forces of comparable interaction strength, the mean-field contributions to the total energy almost cancel each other out and become of the same order as low-energy quantum fluctuations. Their sudden prominence has given rise to the discovery of quantum droplets and supersolids that have been recently studied at length both in experiment and theory [5]. In three dimensions, one can easily add the effective term describing quantum fluctuations, called the Lee-Huang-Yang (LHY) correction, to the GPE leading to its extended version both for Bose-Bose mixtures [6] and dipolar Bose gas [7, 8], that resolves the initial problem. However, for the dipolar case in one or two dimensions, such an approach is more challenging to justify [9].

The widely-used GPE, even supplemented by the LHY correction, becomes unreliable for the strong interaction, especially in lower dimensions where quantum effects are enhanced. A question arises whether there exists a better effective non-linear model that would be useful to study quasi-1D Bose gas also for strongly correlated systems. The simplest system to study is the uniform one and interacting only via short-range repulsive forces. The underlying many-body model describing such a system with N particles is given by the exactly solvable Lieb-Liniger (LL) model [10–12]. Nowadays, the LL model is a test bed for many-body methods, a starting point of subsequent theoretical frameworks (like Luttinger liquid), but also an active area of research in mathematical physics [13, 14].

Although the LL model describes uniform repulsive 1D Bose gas completely, an effective framework, somehow similar to the GPE, has been sought that would be suitable also for strongly correlated systems with additional trapping potential or different interaction type. In the extreme case of trapped 1D gas in the Tonks-Girardeau limit, Kolomeisky et al. [15] already proposed a non-linear equation with higher-order nonlinearity than the GPE. Despite the initial critics by Girardeau and Wright [16], the equation was generalized in [17, 18] to any interaction strength and successfully applied to a problem of an expanding 1D cloud. Similar extensions served to study ground state properties as well as collective excitations of strongly interacting gas in a harmonic trap [19, 20] and dynamics of shock waves [21, 22]. Finally,

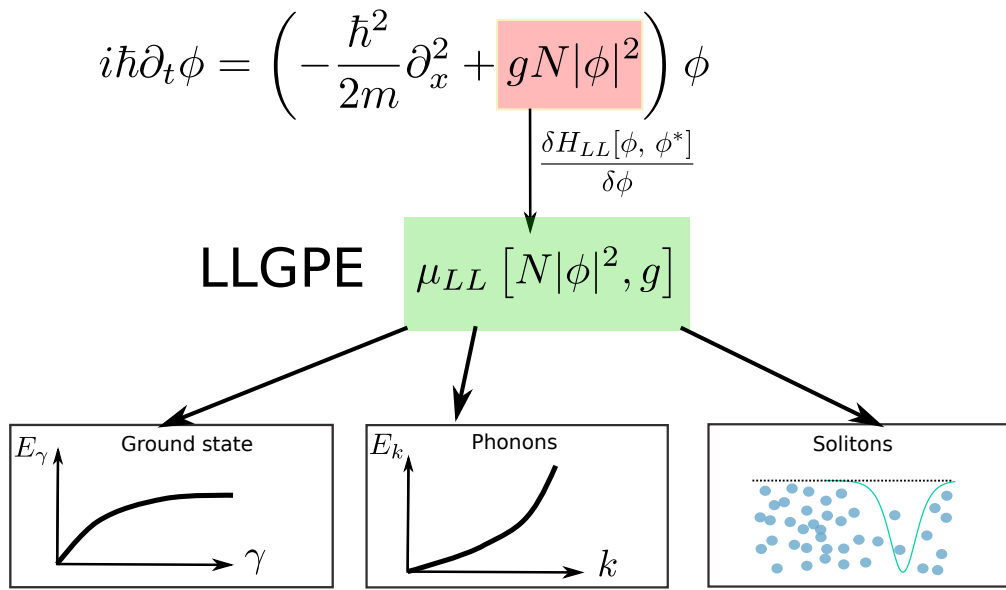


Figure 1: Graphical abstract: We describe a 1D Bose gas, using equation called here LLGPE. LLGPE differs from GPE only by the interaction energy term, after explanation given in this paper, is replaced with the chemical potential of the Lieb-Liniger model. We study the energy of the ground state, dispersion relations of elementary excitations and properties of solitons using LLGPE. We benchmark our findings with GPE and the exact solutions of the Lieb-Liniger model, in all interaction regimes, from the weakly interacting gas up to the Tonks-Girardeau limit.

alternatives of the GPE for strongly interacting dipolar systems have been proposed [23, 24] and have already shown usefulness in timely topics like dipolar quantum droplets [24, 25].

To assess the validity scope of the effective approach employed in this work, we focus on the system described by the LL model. We will benchmark the ground state and its elementary excitations inferred from the effective non-linear approach [15, 18, 24], called here the Lieb-Liniger Gross-Pitaevski equation (LLGPE), against the corresponding solutions of the LL model [10, 11] to test the validity range of the former. Our equation has the form of the GPE but with the nonlinearity from the exact results for the Lieb-Liniger model, see Fig. 1. It has appeared in the literature under the names the Modified Non-linear Schrödinger Equation [26] and the Generalized Non-linear Schrödinger Equation [27]. Here, we will focus on two branches of elementary excitations in the LL that particle (type-I) and hole (type-II) modes correspond to phonons and solitons respectively. The figures of merit are their dispersion relations and, for the type-II excitations, their spatial dependence. We will discuss the interpretation of solitons as the many-body excitations for strong and intermediate interaction strength. In this way, we will test the scope of the non-linear model, which is the cornerstone of the quantum droplet description employed in [24] and an analysis of breathing modes in [25].

The paper is organized as follows. In Sec. 2 we introduce all important models: the LL model, the standard non-linear equation and finally the main subject of this paper, i.e. the generalized non-linear equation. In Sec. 3 and 4 we discuss quasiparticles and solitons, respectively. In Conclusions we predict the scope of validity of the generalized equation.

2 Models

In this Section, we introduce different models of N bosons moving along a circle of length L and interacting via delta potential $V(x) = g\delta(x)$, where x is the distance between particles and g is the coupling strength.

The fundamental model is expressed by the following many-body Hamiltonian

$$\hat{H} = -\frac{\hbar^2}{2m} \sum_{j=1}^N \partial_{x_j}^2 + g \sum_{\substack{j, l \\ j < l}}^N \delta(x_j - x_l), \quad (1)$$

where x_j denotes position of the j -th particle. The Hamiltonian (1) equals to the Lieb-Liniger Hamiltonian, with physical constants written explicitly.

The seminal papers of Lieb and Liniger [10, 11] present the general form of all eigenstates of the Hamiltonian (1) in the case of repulsive interactions, i.e. $g > 0$. A useful dimensionless parameter is

$$\gamma := \frac{m}{\hbar^2} \frac{g L}{N} \quad (2)$$

known as the Lieb parameter. In particular, the energy of the ground state E_0 in the thermodynamic limit ($N \rightarrow \infty$, $L \rightarrow \infty$, $N/L = \text{const}$) is given by

$$E_0[N, L] = \frac{\hbar^2}{2m} \frac{N^3}{L^2} e_{\text{LL}}(\gamma), \quad (3)$$

that defines the pressure [28]:

$$P_{\text{LL}}[N/L] = -\frac{\partial E_0[N, L]}{\partial L} = \frac{\hbar^2}{2m} \frac{N^3}{L^3} (2e_{\text{LL}}(\gamma) - \gamma e'_{\text{LL}}(\gamma)), \quad (4)$$

and the chemical potential:

$$\mu_{\text{LL}}[N/L] = \frac{\partial E_0[N, L]}{\partial N} = \frac{\hbar^2}{2m} \frac{N^2}{L^2} (3e_{\text{LL}}(\gamma) - \gamma e'_{\text{LL}}(\gamma)). \quad (5)$$

as well. Here, $e_{\text{LL}}(\gamma)$ does not have a known explicit analytical form^{1,2}. Note that, unlike the total energy, the pressure and chemical potential as intensive properties depend only on the ratio N/L .

Unfortunately, the many-body eigenstates of the LL model [10] are often impractical to use straightforwardly due to the number of permutations of the N -particle bosonic state. One has to resort to approximate models, from which the easiest one is the GPE. A typical derivation of GPE is based on an Ansatz in the form of the Hartree product, in which the many-body solution of the Schrödinger equation $\psi(x_1, \dots, x_N, t)$ is approximated by a product state $\prod_{j=1}^N \phi(x_j, t)$. The LL Hamiltonian (1) averaged in such Ansatz gives the mean energy³:

$$E_{\text{GPE}}[\phi] = \frac{N}{2} \int dx \left[\frac{\hbar^2}{m} \left| \frac{d\phi}{dx} \right|^2 + gN|\phi|^4 \right]. \quad (6)$$

The least action principle applied to the energy functional above leads to the Gross-Pitaevskii equation for an optimal orbital $\phi(x, t)$:

$$i\hbar \partial_t \phi(x, t) = \left(-\frac{\hbar^2}{2m} \partial_x^2 + gN|\phi(x, t)|^2 \right) \phi(x, t). \quad (7)$$

As the Ansatz assumes a separable state, it has to fail if atoms are quantum correlated. In particular, one cannot justify Eq. (7) for strongly repulsive atoms. On the other hand, there might exist another model not based on such an Ansatz that would be able to capture the essentials of the system even in the strongly interacting regime. Indeed, such models for fermions are being derived routinely in the frame of the density functional theory.

Here, we use the hydrodynamical approach to extend approximate models beyond weak interactions. The classical hydrodynamic equations⁴ read:

$$\frac{\partial}{\partial t} \rho + \frac{\partial}{\partial x} (\rho v) = 0 \quad (8)$$

$$\frac{\partial}{\partial t} v + v \frac{\partial}{\partial x} v = \frac{1}{m\rho} \frac{\partial}{\partial x} P, \quad (9)$$

where $m \cdot \rho(x, t)$, with $\int \rho(x, t) = N$, is the gas density, $v(x, t)$ denotes the velocity field, and $P(x, t)$ indicates pressure. We treat an atomic cloud as composed of small 'volume' elements, which are still large enough that comprise many particles. Following Dunjko, we assume local equilibrium, i.e. in each 'volume' element the energy density, pressure and chemical potential are fixed by the corresponding values of the many-body energy of the ground state. (3) (after replacing N/L by $\rho(x, t)$ everywhere).

¹The values of $e_{\text{LL}}(\gamma)$ can be determined by solving the Fredholm equations given in [10] (where it is denoted as $e(\gamma)$ without subscripts)

²Please do not confuse with e_{LL} introduced in Ref. [24], where it had a meaning of the total energy per volume unit. Moreover, it used rough approximation of the total energy

³We consider $N \gg 1$ therefore we replace $N - 1$ with N .

⁴The quantum hydrodynamic equation might consist of the quantum pressure term. Its role and flows in the considered system are discussed in [21]

Comparing (4) and (5), one may check by direct calculation that the Euler equation (9) may be rewritten as:

$$\frac{\partial}{\partial t} v + v \frac{\partial}{\partial x} v = -\frac{1}{m} \frac{\partial}{\partial x} (\mu_{\text{LL}} [\rho]) \quad (10)$$

Note that Eq. (10) may be derived in an alternative, more intuitive way. Suppose the fluid consists of many particles and consider the trajectory $(x(t), t)$ of one of them. As the potential energy for the particle at any point is given by a chemical potential μ_{LL} , one has directly from Newton's law of motion:

$$\frac{d}{dt} mv(x(t), t) = -\frac{\partial}{\partial x} \mu_{\text{LL}} [\rho(x, t)], \quad (11)$$

which, after a straightforward unravelling of $\frac{d}{dt}$, gives Eq. (10).

Introducing

$$\phi(x) = \sqrt{\rho/N} e^{i\varphi} \quad (12)$$

with $\hbar \partial_x \varphi = mv$, the two hydrodynamical equations (8),(10) can be written, up to a quantum pressure term, in a compact form [21,29]:

$$i\hbar \frac{\partial}{\partial t} \phi = -\frac{\hbar^2}{2m} \frac{\partial^2 \phi}{\partial x^2} + \mu_{\text{LL}} [N|\phi|^2] \phi, \quad (13)$$

with

$$\mu_{\text{LL}} [N|\phi|^2] = \frac{\hbar^2}{2m} N^2 |\phi|^4 \left(3e_{\text{LL}} \left(\frac{\kappa}{N|\phi|^2} \right) - \frac{\kappa}{N|\phi|^2} e'_{\text{LL}} \left(\frac{\kappa}{N|\phi|^2} \right) \right) \quad (14)$$

where $\kappa := \frac{gm}{\hbar^2}$ denotes a parameter of inverse length dimension.

The equation (13) is our main subject of interest. In particular, one can rewrite it also as

$$i\hbar \frac{\partial}{\partial t} \phi = \frac{\delta \mathcal{H}_{\text{LL}}[\phi, \phi^*]}{\delta \phi^*}, \quad (15)$$

where

$$\mathcal{H}_{\text{LL}}[\phi, \phi^*] := \frac{\hbar^2}{2m} \left| \frac{d\phi}{dx} \right|^2 + \frac{\hbar^2}{2m} N^2 |\phi|^6 e_{\text{LL}} \left(\frac{\kappa}{N|\phi|^2} \right) \quad (16)$$

is the energy density. Thus the LLGPE can be derived using the least action principle for the energy functional:

$$E[\phi] = N \int dx \mathcal{H}[\phi, \phi^*] = \frac{N\hbar^2}{2m} \int dx \left[\left| \frac{d\phi}{dx} \right|^2 + N^2 |\phi|^6 e_{\text{LL}} \left(\frac{\kappa}{N|\phi|^2} \right) \right], \quad (17)$$

Notably, ϕ does not have interpretation of a macroscopically occupied orbital, as in the derivation of GPE.

The resulting dynamical equation (13) coincides with the GPE for $\gamma \ll 1$, and the equation proposed in [15] for $\gamma \rightarrow \infty$. From the construction, the minimal value of the energy function (17), obtained for the constant function

$$\phi_{\text{GS}}(x) = \frac{1}{\sqrt{L}} \quad (18)$$

equals to the actual ground state energy $E_0[N, L]$, for any interaction strength γ . The ground state of the GPE equals to the function (18) also, but its GPE energy, $E_{\text{GPE}}[\phi_{\text{GS}}] = N^2 g/L$, approximates E_0 well in the weakly interacting regime only.

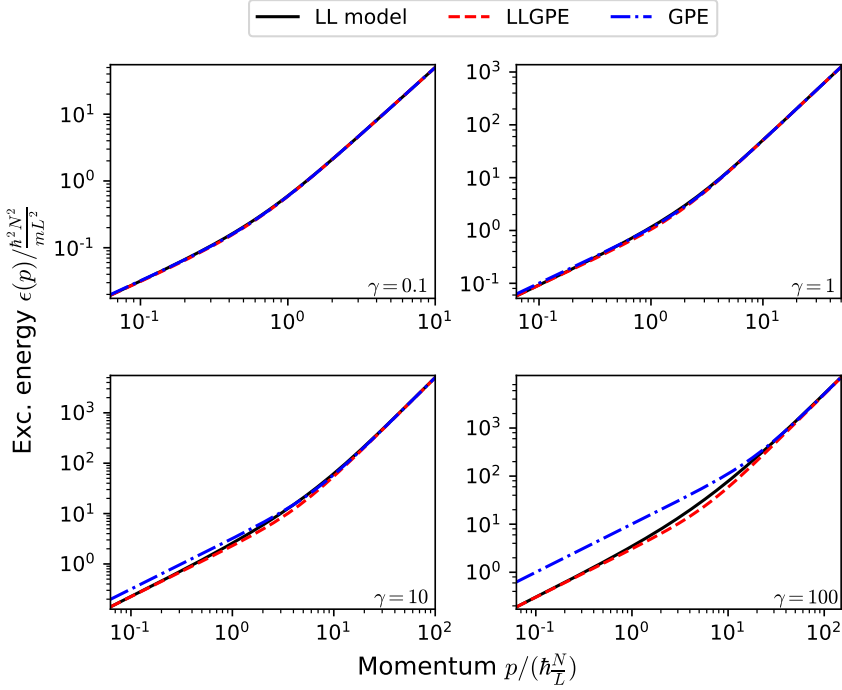


Figure 2: Energy of type-I excitations as a function of the momentum for different values of the interparticle interaction γ . Following Lieb's recipe [11], excitation energies for the LL model were obtained directly from solutions of the Bethe equations for $N = 100$ particles. On the other hand, red and blue dashed lines correspond to the excitation spectrum calculated from linearization of the GPE (7) and LLGPE, respectively.

In the following sections, we will benchmark the underlying Lieb-Liniger model with the approximated ones, the GPE and LLGPE, elaborating the advantages of the latter. In our numerical analysis, we approximate the function e_{LL} , which does not have a known exact and compact form, with a very accurate approximation, presented in [30], and repeated here in the Appendix A.

3 Phonons and quasiparticles

Sound propagation, superfluidity, normal modes, stiffness – all these depend on the quasiparticles properties in a many-body system. In the case of weak interaction strength, the dispersion relation of excitations was computed by Bogoliubov [31], before the general solution of Lieb. The very notion of quasiparticles, natural in the approximated treatment of Bogoliubov, needed a new formulation in the exact many-body theory. Surprisingly, the elementary excitations defined by E. Lieb form two excitation branches instead of one. One of them, the branch of the so-called type-I excitations, has almost the same dispersion relation $E_I(p)$ as the Bogoliubov modes (in the weak interaction regime). For low momenta, their energy scales linearly with momentum,

$$E_I(p) \xrightarrow{p \rightarrow 0} v |p|, \quad (19)$$

where v stands for the speed of sound. These excitations, responsible for superfluidity, are the carriers of sound and are known as phonons.

The fast quasiparticles have the dispersion relation of free particles:

$$E_I(p) \xrightarrow{p \rightarrow \infty} p^2/(2m). \quad (20)$$

As shown in Ref. [32], linearization around the ground state in the frame of the GPE leads to the same dispersion relation as using Bogoliubov quasiparticles. Therefore, we recall and apply this method to both approximate models, the GPE and LLGPE, to trace the differences between, similarly to Ref. [19].

Linearization. — We consider a small perturbation to the stationary solution (18). Following Ref. [33], we restrict ourselves to linearized dynamics and propose an Ansatz for a time-dependent solution in the form:

$$\phi(x, t) = \left(\frac{1}{\sqrt{L}} + \delta\phi(x, t) \right) e^{-i\mu_{\text{LL}}[N/L]t/\hbar}, \quad (21)$$

where $\delta\phi(x, t) = \sum_p u_p(x)e^{-i\epsilon_p t/\hbar} + v_p^*(x)e^{i\epsilon_p t/\hbar}$ is assumed to be a small correction to the stationary solution (18). Hence, after substituting the Ansatz to the LLGPE, we keep terms at most linear in $\delta\phi$ and obtain

$$i\hbar\partial_t\delta\phi = \left[-\frac{\hbar^2}{2m}\partial_x^2 + mv_{\text{LL}}^2[N/L] \right] \delta\phi + mv_{\text{LL}}^2[N/L]\delta\phi^* \quad (22)$$

where $v_{\text{LL}}[N/L] = \frac{\hbar N}{mL} \sqrt{3e_{\text{LL}}(\gamma) - 2\gamma e'_{\text{LL}}(\gamma) + \frac{1}{2}\gamma^2 e''_{\text{LL}}(\gamma)}$ determines an exact expression for the speed of sound in LL model [11, 34]. We plug our ansatz for $\delta\phi(x, t)$ getting:

$$\epsilon_p u_p(x) = \left(-\frac{\hbar^2}{2m}\partial_x^2 + mv_{\text{LL}}^2[N/L] \right) u_p(x) + mv_{\text{LL}}^2[N/L]v_p(x) \quad (23)$$

$$-\epsilon_p v_p(x) = \left(-\frac{\hbar^2}{2m}\partial_x^2 + mv_{\text{LL}}^2[N/L] \right) v_p(x) + mv_{\text{LL}}^2[N/L]u_p(x). \quad (24)$$

Owing to the translational invariance of our system, we consider $u_p(x) = u_p e^{ipx/\hbar}$ and $v_p(x) = v_p e^{ipx/\hbar}$ simplifying our equations to the form:

$$\epsilon_p u_p = \frac{p^2}{2m} u_p + (u_p + v_p)mv_{\text{LL}}^2[N/L] \quad (25)$$

$$-\epsilon_p v_p = \frac{p^2}{2m} v_p + (u_p + v_p)mv_{\text{LL}}^2[N/L]. \quad (26)$$

We solve these equations, finally obtaining the excitation spectrum:

$$\epsilon(p) = \sqrt{(v_{\text{LL}}[N/L]p)^2 + \left(\frac{p^2}{2m}\right)^2}. \quad (27)$$

The formula (27) is the main result of this section. In the low momenta limit, one gets $\epsilon(p) \xrightarrow{p \rightarrow 0} v_{\text{LL}}[N/L]|p|$, i.e. the phononic relation with the correct speed of sound, the same as in the many-body approach. Interestingly, we recover also the correct limit (up to second

order) for large momenta (cf. (20)). Thus the linearization of the LLGPE gives a dispersion relation that coincides with the dispersion relation of type-I elementary excitations at low and high energy limit and for any interaction strength. In Fig. 2, we show a comparison between (27) and the exact many-body solutions. The deviations are present only for the intermediate momenta. For completeness, we also show the dispersion relation based on the linearization of GPE. It reads $\epsilon_{\text{GP}}(p) = \sqrt{(v_{\text{GP}}[N/L]p)^2 + \left(\frac{p^2}{2m}\right)^2}$, with a modification in the speed of sound which equals $v_{\text{GP}}[N/L] := \sqrt{gN/mL}$ and tends to infinity in the Tonks-Girardeau limit.

The results presented in this section show how well the LLGPE works concerning type-I excitations for all interaction regimes. This leads us to more subtle questions about non-linear effects. Such effects appear naturally in the GPE but are more difficult to control in the frame of the many-body approach, which is based on the linear equation. In the next sections, we shall focus on solitons and their relations with the type-II elementary excitations.

4 Solitons

The GPE appears to be very convenient to study non-linear phenomena, like solitons. Generally speaking, a soliton is a solution of a non-linear equation in the form of a moving wave, $\phi_S(x, t) = \phi_S(x - v_s t)$, that preserves its shape in dynamics due to the balance between kinetic energy and nonlinearity. In the case of the GPE with repulsive interaction, a soliton has a form of a density dip, as shown by a blue dashed line in Fig. 3. Such solitonic dips, predicted by the GPE, were demonstrated experimentally [2, 3]. Here, we will focus on a special case, namely solitons with the density dip touching 0, called the *black solitons*.

4.1 Comparison between solitons of GPE and LLGPE

As discussed above, the linearization of the LLGPE leads to the correct speed of sound in the 1D gas of bosons with short-range interaction, even for the intermediate and strong interaction regime. A natural question arises whether the LLGPE has a solitonic solution beyond the weakly interacting regime.

Here, following the reasoning presented in Ref. [35], we find candidates for solitons in LLGPE numerically for any interaction strength, as the minimal energy states constraint to a π jump of phase at the origin. We tested numerically that these states do not move and preserve their shape in dynamics, as solitons should do. The technical details of our method and references to our codes are given in Appendix B. The results for the LLGPE are shown in Fig. 3 with the solid black lines, together with the GPE solitons (blue dashed lines). The width of a GPE soliton, which is of the order of the healing length $\xi := \hbar/\sqrt{mNg/L}$, vanishes in the limit of large g . This is an unphysical effect: in reality, the gas reaches the Tonks-Girardeau limit, at which the further increase of interaction strength does not affect the system anymore. In the LLGPE, this saturation effect is accounted for by the relation $e_{\text{LL}}(\gamma) \xrightarrow{\gamma \rightarrow \infty} \pi^2/3$, and the width of LLGPE solitons converges to a constant. As shown in Fig. 3, already for $\gamma = 100$, the LLGPE soliton is indistinguishable from the solitons that are analytically derived in the limit $\gamma \rightarrow \infty$ (red dashed line) [15].

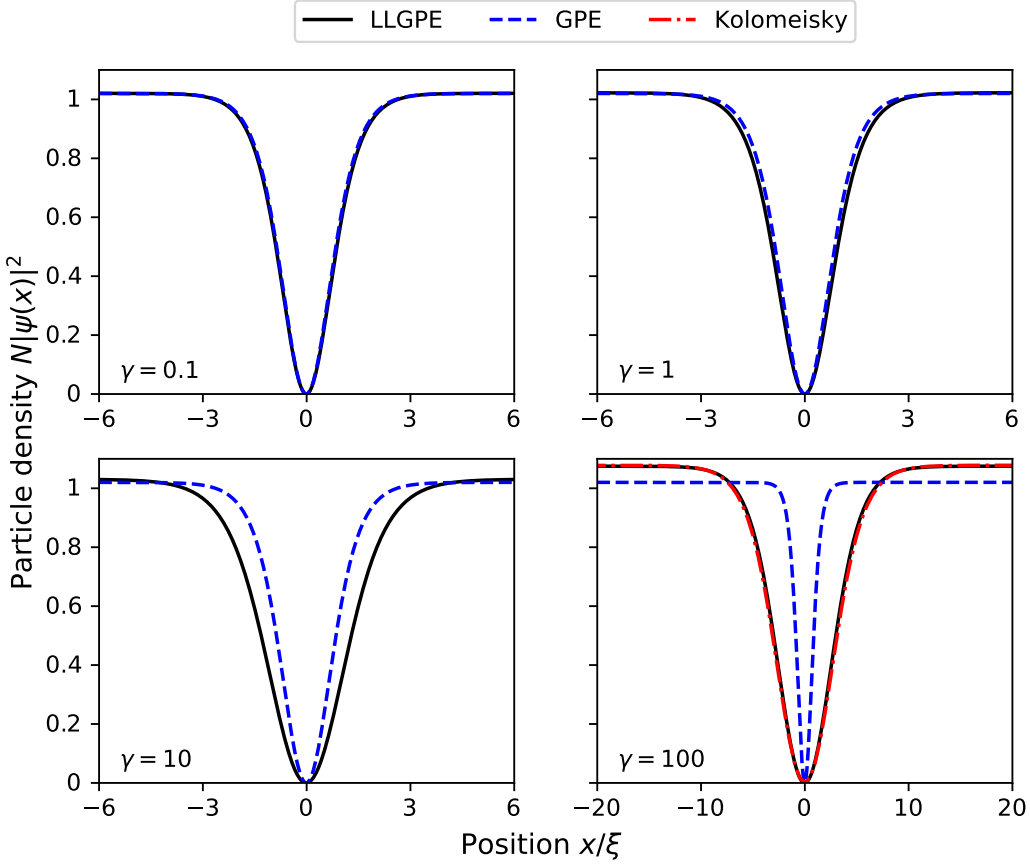


Figure 3: Black soliton density profiles for different equations and interaction strengths. Note the GPE and LLGPE solutions for $\gamma = 0.1$ as well as LLGPE and Kolomeisky (cf. Ref. [15]) solutions for $\gamma = 100$ overlap each other. In all cases the box size $L = 100\xi$, where ξ is the healing length (which corresponds to $N = 100\sqrt{1/\gamma}$).

4.2 Comparison between solitons and the type-II excitations

It was observed in Ref. [36] that for weak interactions, the GPE solitons have the same dispersion relation as the many-body eigenstates forming the second branch of elementary excitations in the solution of Lieb called in the literature yrast states or type-II excitations or the lowest energy states at fixed momentum. This coincidence was rather unexpected: why the dispersion relation of the solutions of a dynamical, non-linear GPE should match the dispersion of some static solutions of the linear many-body model, distinguished by E. Lieb as the type-II elementary excitations?

There has been a lot of effort devoted to understanding better this relation [35,37–39,39–47]. It has been pointed out that the GPE soliton emerges in the high order correlation function computed for the type-II excitation [41, 42]. The other observation points that the solitonic shape appears also in the single-body reduced density matrix evaluated in the appropriate superpositions of the type-II excitations [43–47]. These two different viewpoints were recently unified in Ref. [35]. The agreement holds, however, for weak interactions only, where the GPE

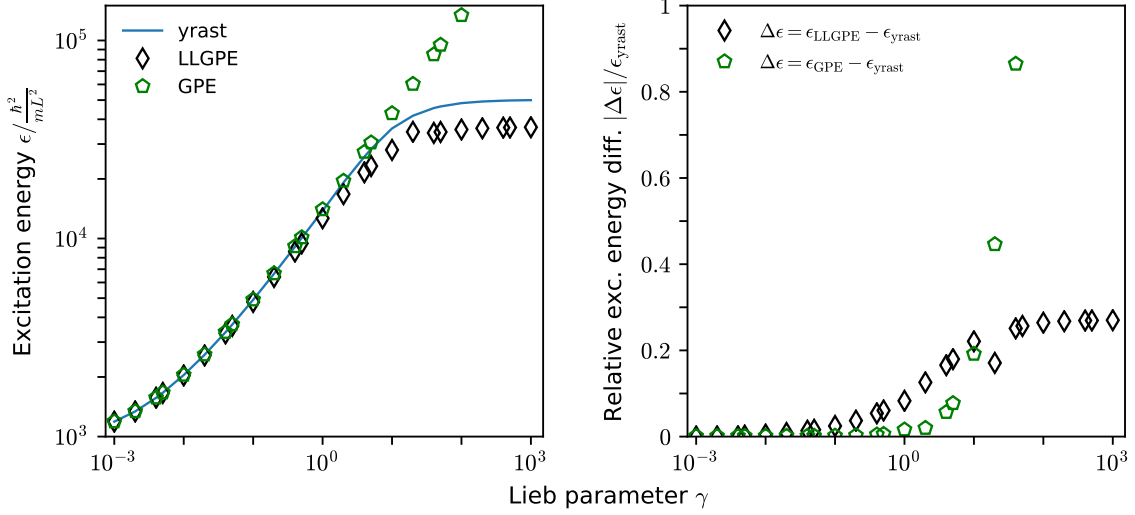


Figure 4: Left: Yrast state excitation energy in the Lieb-Liniger model (blue line) vs dark soliton excitation energy obtained with the LLGPE (black diamonds) and the GPE (green pentagons) as a function of the Lieb parameter γ . Right: Relative excitation energy $\Delta\epsilon$ of dark solitons within the LLGPE (black diamonds) and GPE (green pentagons). Parameters used in all simulations: $N = 100$.

is reliable. Here, we address a question whether the relation between solitons and the type-II excitations remains valid for stronger interaction, provided that we use the LLGPE solitons for comparison.

In Fig. 4, we compare the energy of the black GPE and LLGPE solitons with the energies of the type-II excitations evaluated from the exact solution [11] for $N = 100$ particles. For comparison, we used the type-II excitations with the total momentum $\hbar\pi N/L$ that has the same momentum per atom as a black soliton. As before, we present the excitation energy being the total energy of the GPE (6) or the LLGPE (17) soliton reduced by the energy of the ground state⁵. The excitation energy of GPE solitons, marked with green hexagons, tends to the infinity with increasing γ . This is a residue of the vanishing width of the GPE soliton that gives a simple estimation of their kinetic energy by $\frac{\hbar^2}{mw^2}$, where w is the soliton width. In the strong interaction limit, the excitation energy of the LLGPE solitons converges to a constant, because the system enters the Tonks-Girardeau phase. The latter dispersion relation qualitatively agrees with the dispersion relation of the type-II excitation, although differences are clearly visible. We show the discrepancies between the energies in the right panel of Fig. 4. The figure shows that in the considered example ($N = 100$), there are significant differences in the relative energies of LLGPE solitons and the type-II excitations, which reaches up to 25% in the Tonks-Girardeau limit. Importantly, this divergence is not an artefact of the small number of atoms used in the comparison. In fact, in the thermodynamic limit and for $\gamma \rightarrow \infty$, the excitation energy of the yrast state equals $E_{\text{yrast}} - E_{\text{GS}} = \frac{\pi^2 \hbar^2 N^2}{2mL^2}$, whereas the LLGPE soliton has the energy equal to $\frac{\pi^2 \hbar^2 N^2}{2mL^2} [\sqrt{3} \log(2 + \sqrt{3})/\pi]$ [15]. That gives relative difference between energies around 28%. For the discrepancy is substantial, we examine closer a relation between these excitations studying their spatial dependence.

⁵The subtracted ground state energy differs between the GPE and the LLGPE.

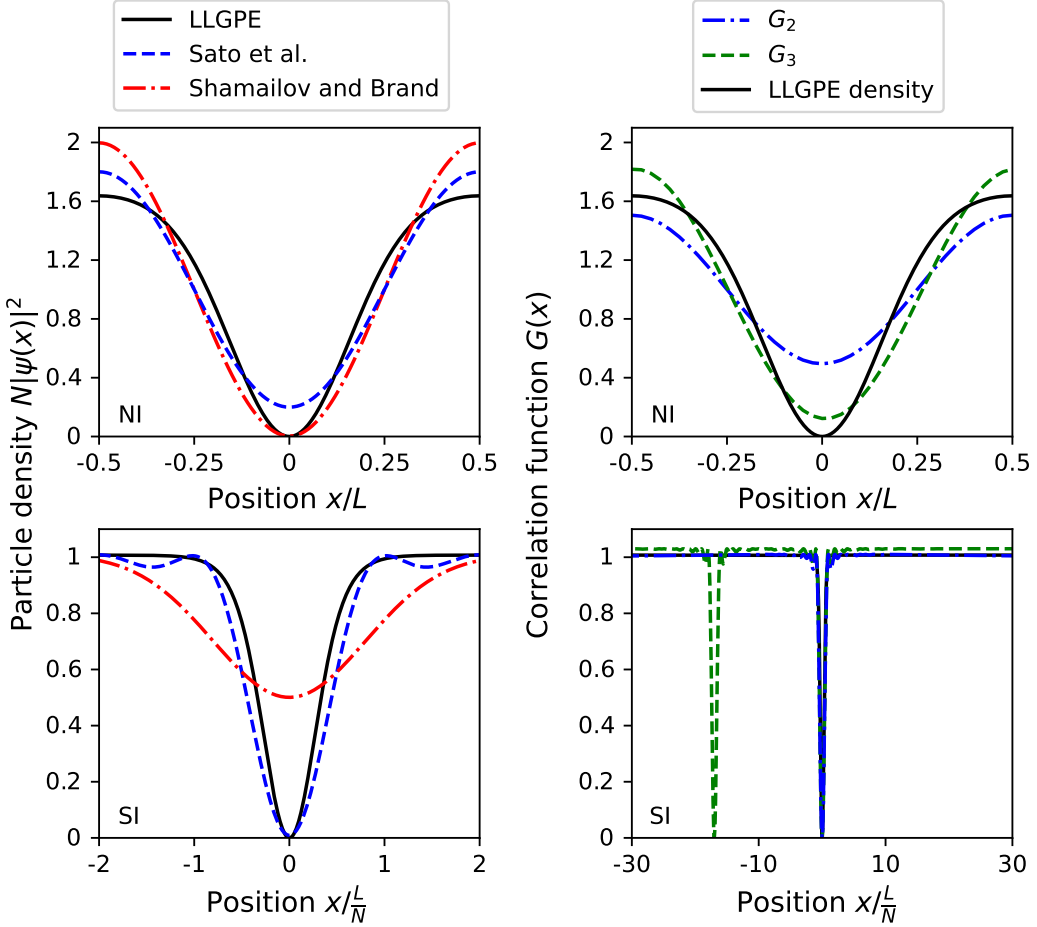


Figure 5: Left panels: Single particle density of the yrast state superpositions (Sato et al. - based on [45], Shamailov and Brand - based on [47] with dyspersion $\Delta P = 0.2\hbar\pi N/L$ used to generate a Gaussian superposition). Right panels: G_2 and G_3 correlation functions evaluated for the yrast state with the total momentum $\hbar\pi N/L$. NI - non-interacting gas, SI - strongly interacting gas ($\gamma \rightarrow \infty$). The G_2 function, one dip in G_3 and the LLGPE solution overlap each other in the strong interaction limit. The length scales used on the horizontal axes reflect that the soliton width depends only on L in the non-interacting regime, and only on L/N in the strongly interacting regime.

Due to the translational symmetry, the single body density of any eigenstate of the LL model, including the type-II elementary excitations, is uniform. To reveal solitons, one can either look at the typical relations between atoms' positions in this eigenstate, for instance, using its correlation functions or break the translation symmetry, for instance, studying a wavepacket of the type-II excitations instead of a single one. In Fig. 5, we recapitulate findings of these two approaches at two extreme regimes: in the limit of non-interacting gas (NI) and the strong-interaction regime (SI). In all panels, we also present LLGPE black solitons marked by a solid black line. The left panels of Fig. 5 show a comparison between the density of the LLGPE soliton and the single-body densities of superpositions of the type-II excitations, as studied in Refs. [43, 45, 47]. These results are not unique in the sense that the reduced density

depends on the choice of the superposition.

The right panels of Fig. 5 present benchmarks between LLGPE solitons and

$$G_m(x_m|x_1, \dots, x_{m-1}) := \mathcal{N} \left\langle \prod_{i=1}^m \hat{\Psi}^\dagger(x_i) \prod_{i=1}^m \hat{\Psi}(x_i) \right\rangle, \quad (28)$$

which is the probability density of measuring m -th particle at a position x_m provided that $m-1$ particles has been already detected at the random points x_1, \dots, x_{m-1} , and \mathcal{N} stands for a normalization factor. Here, we show results for $m = 2$ and $m = 3$ only. It has been checked that for weak interactions G_m coincides with a soliton profile for sufficiently large m [35, 41]. A situation in the TG limit (bottom right of Fig. 5) is very different. In the limit $\gamma \rightarrow \infty$, the correlation functions assume a simple structure. Owing to the fermionization, the atoms have to be at different places. Thus the probability of finding the m -th particle, provided that $m-1$ particles were already measured, has zeros at the locations of already measured particles. Therefore, although the LLGPE soliton seems similar to the G_2 function of the yrast state, it has to differ from the higher order correlation functions that have m local minima and not a single one likewise the soliton. Actually, the fact that the LLGPE soliton is close to G_2 of the fermionized gas is alarming in the context of the hydrodynamical origin of the LLGPE.

5 Validity range of LLGPE and solitons

The LLGPE equation derives from the hydrodynamical description, assuming that locally the gas is at equilibrium. However, what *locally* means has to be specified. In the theory of continuous media, one introduces fluid elements consisting of many atoms but spanned over the lengths much shorter than the length scale associated with the density changes. It means that we should restrict our analysis to such solitons for which the latter length, of the order of the soliton width w , is much larger than the typical distance between particles, here roughly approximated by L/N . The width w can be estimated from the condition that the kinetic energy of a soliton, which is of the order of $\hbar^2/(2mw^2)$, balances the non-linear term in Eq. (13), which is of the order of $\mu_{\text{LL}}[N/L]$. This balance leads to an estimate $w \approx \hbar/\sqrt{2m\mu_{\text{LL}}[N/L]}$. In the case of the weakly interacting limit, i.e. $\mu_{\text{LL}} \approx gN/L$, one gets $w_{\text{GPE}} \approx \hbar/\sqrt{2mgN/L}$, which gives the correct length scale of the GPE soliton width. The hydrodynamical analysis relies on the assumption $w \gg L/N$, which can be expressed as $1 \gg 2\gamma$. Indeed, these qualitative considerations are confirmed by the numerical analysis of the solitonic width illustrated in Fig. 6. The width of the GPE soliton, shown with the dashed green line crosses the typical distance between atoms L/N (blue line) around $\gamma = 1/2$. Apparently, the situation does not significantly change for LLGPE solitons (black dots).

The qualitative discussion of the length scales leads to the conclusion that the solitons presented in the previous section fulfil the assumptions underlying the LLGPE only for weakly interacting gas. In particular, the analytical solutions given in Ref. [15] can exceed the validity range of the LLGPE. In the Tonks-Girardeau limit considered in Ref. [15], the solitonic width equals the typical distance between particles that, owing to the fermionization, is of the order of L/N . In that situation, one cannot define elements of fluid consisting of many atoms with a smooth density profile as assumed in the derivation of the LLGPE. This will be also the case of other states involving length scales shorter than interparticle distance, for example,

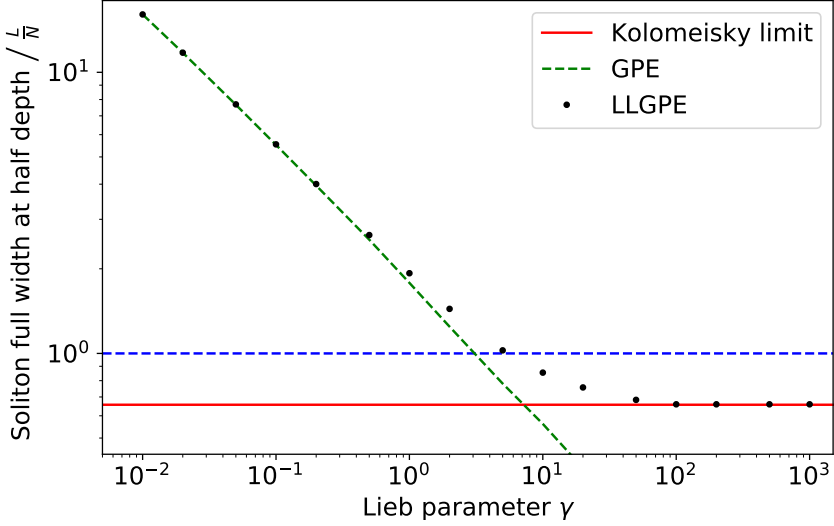


Figure 6: Widths of black LLGPE (black dots) and GPE (green dashed line) solitons found with the ITE method as a function of the Lieb parameter γ . The dashed blue line corresponds to the average interparticle distance L/N and the solid red one to the Kolomeisky limit for $\gamma \rightarrow \infty$ (cf. [15]).

two interfering atomic clouds [16] or shock waves [21]. The question of whether solitons exist in the intermediate and strongly interacting regimes may be difficult to resolve on theoretical grounds. We leave the question about their existence open as a challenge for experimentalists.

6 Conclusions

The purpose of this work has been to benchmark the LLGPE on a well-studied case, a gas trapped in a 1D box with the periodic boundary conditions. In introducing the LLGPE equation, we invoke the hydrodynamic interpretation. We expect that the equation works in cases where the gas density is slowly varying in space. Indeed, the linearization of the LLGPE leads to the analytical formula for phononic spectra that coincides with the exact formulas known for type-I excitations of the Lieb-Liniger model, even in the limit of infinite interactions. We also find solitonic solutions of the LLGPE and compare their dispersion relation and the spatial dependence to type-II excitations of the Lieb-Liniger model forming a 'solitonic' branch. The correspondence between LLGPE solitons and type-II excitations is limited to weak interaction $\gamma \lesssim 1$. For stronger interaction, the LLGPE solitons do not meet assumptions underlying the LLGPE. The question of whether solitons exist in the 1D gas beyond the weakly interacting regime remains open. The problem might be addressed by experimenters with the technique that was successfully employed for the weakly interacting gas.

To conclude, the LLGPE offers an alternative tool to the GPE, useful in a wide class of smooth solutions even in the strongly interacting 1D Bose gas. One can apply it to a gas

confined by a slowly varying external potential or for atoms interacting via smooth non-local potential.

Acknowledgements

We thank G. Astrakharchik and B. Julia-Diaz for fruitful discussions. Center for Theoretical Physics of the Polish Academy of Sciences is a member of the National Laboratory of Atomic, Molecular and Optical Physics (KL FAMO).

Funding information J.K., M.L., M.M., K.P. acknowledges support from the (Polish) National Science Center Grant No. 2019/34/E/ST2/00289. This research was supported in part by PLGrid Infrastructure.

A Accurate approximations for e_{LL}

In the regime of weak interactions $\gamma < 1$ we have

$$e_{LL}(\gamma) = \gamma - \frac{4}{3\pi}\gamma^{3/2} + \left[\frac{1}{6} - \frac{1}{\pi^2}\right]\gamma^2 - 0.0016\gamma^{5/2} + O(\gamma^3). \quad (29)$$

For intermediate interactions $1 \leq \gamma < 15$

$$e_{LL}(\gamma) \approx \gamma - \frac{4}{3\pi}\gamma^{3/2} + \left[\frac{1}{6} - \frac{1}{\pi^2}\right]\gamma^2 - 0.002005\gamma^{5/2} + 0.000419\gamma^3 - 0.000284\gamma^{7/2} + 0.000031\gamma^4. \quad (30)$$

Finally, nearly the fermionized regime $\gamma \geq 15$

$$\begin{aligned} e_{LL}(\gamma) \approx & \frac{\pi^2}{3} \left(1 - \frac{4}{\gamma} + \frac{12}{\gamma^2} - \frac{10.9448}{\gamma^3} - \frac{130.552}{\gamma^4} + \frac{804.13}{\gamma^5} - \frac{910.345}{\gamma^6} - \frac{15423.8}{\gamma^7} + \right. \\ & \frac{100559.}{\gamma^8} - \frac{67110.5}{\gamma^9} - \frac{2.64681 \times 10^6}{\gamma^{10}} + \frac{1.55627 \times 10^7}{\gamma^{11}} + \frac{4.69185 \times 10^6}{\gamma^{12}} - \\ & \frac{5.35057 \times 10^8}{\gamma^{13}} + \frac{2.6096 \times 10^9}{\gamma^{14}} + \frac{4.84076 \times 10^9}{\gamma^{15}} - \frac{1.16548 \times 10^{11}}{\gamma^{16}} + \\ & \left. \frac{4.35667 \times 10^{11}}{\gamma^{17}} + \frac{1.93421 \times 10^{12}}{\gamma^{18}} - \frac{2.60894 \times 10^{13}}{\gamma^{19}} + \frac{6.51416 \times 10^{13}}{\gamma^{20}} + O\left(\frac{1}{\gamma^{21}}\right) \right). \end{aligned} \quad (31)$$

B Numerical implementation of dark solitons in (LL)GPE

The (LL)GPE (cf. Eq. 7 for GPE and Eq. 15 for LLGPE) is a complex, non-linear partial differential equation. In order to solve it, we use the imaginary time evolution (ITE) method. The wave function ψ is represented on a one-dimensional spatial lattice with N_x fixed points with lattice constant $DX = \frac{L}{N_x}$.

The algorithm is built in such way that we choose an initial guess. We further evolve the initial guess in imaginary time $t \mapsto -i\tau$. It is done with the use of split-step numerical method. The evolution in kinetic energy term is done in the momentum domain, the self-interaction term is calculated in the spatial domain.

No external potential is used. The solution is being found in a box with periodic boundary conditions $\psi\left(\frac{-L}{2}\right) = \psi\left(\frac{L}{2}\right)$.

We use phase imprinting to generate solitonic solutions. In every iteration the wave function is modified in such way that $\arg \psi(x) = \pi \left(\frac{x}{L} + 0.5 \right)$ for $x \in \left(-\frac{L}{2}, 0 \right)$ and $\arg \psi(x) = \pi \left(\frac{x}{L} - 0.5 \right)$ for $x \in \left(0, \frac{L}{2} \right)$. One can easily see that there is a π phase jump for $x = 0$. Moreover, the periodic boundary conditions in terms of phase, i.e. $\arg \psi\left(\frac{-L}{2}\right) = \arg \psi\left(\frac{L}{2}\right)$, are fulfilled.

The resulting soliton profile remains unchanged in course of the real time evolution.

The program implementing the algorithm above is available here: <https://gitlab.com/jakkop/mudge/-/tags/v01Jun2021>. The program uses W-DATA format dedicated to store data in numerical experiments with ultracold Bose and Fermi gases. The W-DATA project is a part of the W-SLDA toolkit [48, 49].

References

- [1] C. J. Pethick and H. Smith, *Bose-Einstein condensation in dilute gases*, Cambridge University Press (2008).
- [2] J. Denschlag, J. E. Simsarian, D. L. Feder, C. W. Clark, L. A. Collins, J. Cubizolles, L. Deng, E. W. Hagley, K. Helmerson, W. P. Reinhardt, S. L. Rolston, B. I. Schneider *et al.*, *Generating solitons by phase engineering of a Bose-Einstein condensate*, *Science* **287**(5450), 97 (2000), doi:10.1126/science.287.5450.97, <https://science.sciencemag.org/content/287/5450/97.full.pdf>.
- [3] S. Burger, K. Bongs, S. Dettmer, W. Ertmer, K. Sengstock, A. Sanpera, G. V. Shlyapnikov and M. Lewenstein, *Dark solitons in Bose-Einstein condensates*, *Phys. Rev. Lett.* **83**, 5198 (1999), doi:10.1103/PhysRevLett.83.5198.
- [4] A. Weller, J. P. Ronzheimer, C. Gross, J. Esteve, M. K. Oberthaler, D. J. Frantzeskakis, G. Theocharis and P. G. Kevrekidis, *Experimental observation of oscillating and interacting matter wave dark solitons*, *Phys. Rev. Lett.* **101**, 130401 (2008), doi:10.1103/PhysRevLett.101.130401.
- [5] F. Boettcher, J.-N. Schmidt, J. Hertkorn, K. Ng, S. Graham, M. Guo, T. Langen and T. Pfau, *New states of matter with fine-tuned interactions: quantum droplets and dipolar supersolids*, *Reports on Progress in Physics* (2020).
- [6] D. Petrov, *Quantum mechanical stabilization of a collapsing Bose-Bose mixture*, *Physical Review Letters* **115**(15), 155302 (2015).
- [7] A. R. Lima and A. Pelster, *Quantum fluctuations in dipolar Bose gases*, *Physical Review A* **84**(4), 041604 (2011).
- [8] A. R. Lima and A. Pelster, *Beyond mean-field low-lying excitations of dipolar Bose gases*, *Physical Review A* **86**(6), 063609 (2012).

- [9] K. Jachymski and R. Oldziejewski, *Nonuniversal beyond-mean-field properties of quasi-two-dimensional dipolar Bose gases*, Phys. Rev. A **98**, 043601 (2018), doi:10.1103/PhysRevA.98.043601.
- [10] E. H. Lieb and W. Liniger, *Exact analysis of an interacting Bose gas. I. The general solution and the ground state*, Phys. Rev. **130**, 1605 (1963), doi:10.1103/PhysRev.130.1605.
- [11] E. H. Lieb, *Exact analysis of an interacting Bose gas. II. The excitation spectrum*, Phys. Rev. **130**, 1616 (1963), doi:10.1103/PhysRev.130.1616.
- [12] E. H. Lieb, R. Seiringer and J. Yngvason, *One-dimensional bosons in three-dimensional traps*, Phys. Rev. Lett. **91**, 150401 (2003), doi:10.1103/PhysRevLett.91.150401.
- [13] J. Mossel and J.-S. Caux, *Exact time evolution of space- and time-dependent correlation functions after an interaction quench in the one-dimensional Bose gas*, New Journal of Physics **14**(7), 075006 (2012), doi:10.1088/1367-2630/14/7/075006.
- [14] M. Panfil and J.-S. Caux, *Finite-temperature correlations in the Lieb-Liniger one-dimensional Bose gas*, Phys. Rev. A **89**, 033605 (2014), doi:10.1103/PhysRevA.89.033605.
- [15] E. B. Kolomeisky, T. J. Newman, J. P. Straley and X. Qi, *Low-dimensional Bose liquids: Beyond the Gross-Pitaevskii approximation*, Phys. Rev. Lett. **85**, 1146 (2000), doi:10.1103/PhysRevLett.85.1146.
- [16] M. D. Girardeau and E. M. Wright, *Breakdown of time-dependent mean-field theory for a one-dimensional condensate of impenetrable bosons*, Phys. Rev. Lett. **84**, 5239 (2000), doi:10.1103/PhysRevLett.84.5239.
- [17] V. Dunjko, V. Lorent and M. Olshanii, *Bosons in cigar-shaped traps: Thomas-Fermi regime, Tonks-Girardeau regime, and in between*, Phys. Rev. Lett. **86**, 5413 (2001), doi:10.1103/PhysRevLett.86.5413.
- [18] P. Öhberg and L. Santos, *Dynamical transition from a quasi-one-dimensional Bose-Einstein condensate to a Tonks-Girardeau gas*, Phys. Rev. Lett. **89**, 240402 (2002), doi:10.1103/PhysRevLett.89.240402.
- [19] Y. E. Kim and A. L. Zubarev, *Density-functional theory of bosons in a trap*, Phys. Rev. A **67**, 015602 (2003), doi:10.1103/PhysRevA.67.015602.
- [20] I. Bouchoule, S. S. Szigeti, M. J. Davis and K. V. Kheruntsyan, *Finite-temperature hydrodynamics for one-dimensional Bose gases: Breathing-mode oscillations as a case study*, Phys. Rev. A **94**, 051602 (2016), doi:10.1103/PhysRevA.94.051602.
- [21] B. Damski, *Formation of shock waves in a Bose-Einstein condensate*, Phys. Rev. A **69**, 043610 (2004), doi:10.1103/PhysRevA.69.043610.
- [22] B. Damski, *Shock waves in a one-dimensional Bose gas: From a Bose-Einstein condensate to a Tonks gas*, Phys. Rev. A **73**, 043601 (2006), doi:10.1103/PhysRevA.73.043601.
- [23] B. B. Baizakov, F. K. Abdullaev, B. A. Malomed and M. Salerno, *Solitons in the Tonks-Girardeau gas with dipolar interactions*, Journal of Physics B: Atomic, Molecular and Optical Physics **42**(17), 175302 (2009), doi:10.1088/0953-4075/42/17/175302.

- [24] R. Oldziejewski, W. Górecki, K. Pawłowski and K. Rzazewski, *Strongly correlated quantum droplets in quasi-1D dipolar Bose gas*, Phys. Rev. Lett. **124**, 090401 (2020), doi:10.1103/PhysRevLett.124.090401.
- [25] S. De Palo, E. Orignac, M. L. Chiofalo and R. Citro, *Polarization angle dependence of the breathing mode in confined one-dimensional dipolar bosons*, Phys. Rev. B **103**, 115109 (2021), doi:10.1103/PhysRevB.103.115109.
- [26] S. Choi, V. Dunjko, Z. D. Zhang and M. Olshanii, *Monopole excitations of a harmonically trapped one-dimensional Bose gas from the ideal gas to the Tonks-Girardeau regime*, Phys. Rev. Lett. **115**, 115302 (2015), doi:10.1103/PhysRevLett.115.115302.
- [27] S. Peotta and M. D. Ventra, *Quantum shock waves and population inversion in collisions of ultracold atomic clouds*, Phys. Rev. A **89**, 013621 (2014), doi:10.1103/PhysRevA.89.013621.
- [28] F. Mancarella, G. Mussardo and A. Trombettoni, *Energy-pressure relation for low-dimensional gases*, Nuclear Physics B **887**, 216 (2014), doi:<https://doi.org/10.1016/j.nuclphysb.2014.08.007>.
- [29] I. Bialynicki-Birula, M. Cieplak and J. Kaminski, *Theory of Quanta*, Oxford University Press (1992).
- [30] G. Lang, F. Hekking and A. Minguzzi, *Ground-state energy and excitation spectrum of the Lieb-Liniger model : accurate analytical results and conjectures about the exact solution*, SciPost Phys. **3**, 003 (2017), doi:10.21468/SciPostPhys.3.1.003.
- [31] N. N. Bogoliubov, *On the theory of superfluidity*, Journal of Physics **11**, 23 (1947), doi:10.1103/PhysRevA.79.063616.
- [32] Y. Castin, *Bose-Einstein Condensates in Atomic Gases: Simple Theoretical Results*, In *Coherent atomic matter waves*, pp. 1–136. Springer, Berlin, Germany, ISBN 978-3-540-41047-8, doi:10.1007/3-540-45338-5_1 (2002).
- [33] L. P. Pitaevskii and S. Stringari, *Bose-Einstein Condensation*, International Series of Monographs on Physics. Clarendon Press (2003).
- [34] Z. Ristivojevic, *Excitation spectrum of the Lieb-Liniger model*, Phys. Rev. Lett. **113**, 015301 (2014), doi:10.1103/PhysRevLett.113.015301.
- [35] W. Golletz, W. Górecki, R. Oldziejewski and K. Pawłowski, *Dark solitons revealed in Lieb-Liniger eigenstates*, Phys. Rev. Research **2**, 033368 (2020), doi:10.1103/PhysRevResearch.2.033368.
- [36] P. P. Kulish, S. V. Manakov and L. D. Faddeev, *Comparison of the exact quantum and quasiclassical results for a nonlinear Schrödinger equation*, Theoretical and Mathematical Physics **28**(1), 615 (1976), doi:10.1007/BF01028912.
- [37] R. Kanamoto, L. D. Carr and M. Ueda, *Topological winding and unwinding in metastable Bose-Einstein condensates*, Phys. Rev. Lett. **100**, 060401 (2008), doi:10.1103/PhysRevLett.100.060401.

- [38] R. Kanamoto, L. D. Carr and M. Ueda, *Metastable quantum phase transitions in a periodic one-dimensional Bose gas: Mean-field and Bogoliubov analyses*, Phys. Rev. A **79**, 063616 (2009), doi:10.1103/PhysRevA.79.063616.
- [39] A. D. Jackson, J. Smyrnakis, M. Magiropoulos and G. M. Kavoulakis, *Solitary waves and yrast states in Bose-Einstein condensed gases of atoms*, EPL (Europhysics Letters) **95**(3), 30002 (2011), doi:10.1209/0295-5075/95/30002.
- [40] O. Fialko, M.-C. Delattre, J. Brand and A. R. Kolovsky, *Nucleation in finite topological systems during continuous metastable quantum phase transitions*, Phys. Rev. Lett. **108**, 250402 (2012), doi:10.1103/PhysRevLett.108.250402.
- [41] A. Syrwid and K. Sacha, *Lieb-Liniger model: Emergence of dark solitons in the course of measurements of particle positions*, Physical Review A **92**(3), 032110 (2015).
- [42] A. Syrwid, M. Brewczyk, M. Gajda and K. Sacha, *Single-shot simulations of dynamics of quantum dark solitons*, Physical Review A **94**(2), 023623 (2016).
- [43] E. Kaminishi, R. Kanamoto, J. Sato and T. Deguchi, *Exact yrast spectra of cold atoms on a ring*, Phys. Rev. A **83**, 031601 (2011), doi:10.1103/PhysRevA.83.031601.
- [44] J. Sato, R. Kanamoto, E. Kaminishi and T. Deguchi, *Exact relaxation dynamics of a localized many-body state in the 1D Bose gas*, Phys. Rev. Lett. **108**, 110401 (2012), doi:10.1103/PhysRevLett.108.110401.
- [45] J. Sato, R. Kanamoto, E. Kaminishi and T. Deguchi, *Quantum states of dark solitons in the 1D Bose gas*, New Journal of Physics **18**(7), 075008 (2016), doi:10.1088/1367-2630/18/7/075008.
- [46] E. Kaminishi, T. Mori and S. Miyashita, *Construction of quantum dark soliton in one-dimensional Bose gas* (2018), arXiv:1811.00211.
- [47] S. S. Shamailov and J. Brand, *Quantum dark solitons in the one-dimensional Bose gas*, Phys. Rev. A **99**, 043632 (2019), doi:10.1103/PhysRevA.99.043632.
- [48] G. Włazłowski, K. Sekizawa, M. Marchwiany and P. Magierski, *Suppressed solitonic cascade in spin-imbalanced superfluid Fermi gas*, Phys. Rev. Lett. **120**, 253002 (2018), doi:10.1103/PhysRevLett.120.253002.
- [49] A. Bulgac, M. M. Forbes, M. M. Kelley, K. J. Roche and G. Włazłowski, *Quantized superfluid vortex rings in the unitary Fermi gas*, Phys. Rev. Lett. **112**, 025301 (2014), doi:10.1103/PhysRevLett.112.025301.